**Supplementary information**

**Footnotes**

a. Department of Materials Science and Engineering, University of Sheffield, Sheffield S1 3JD, United Kingdom. E-mail: dawei.wang@sheffield.ac.uk (corresponding author email address)
b. Electronic Materials Research Laboratory, Key Laboratory of the Ministry of Education & International Center for Dielectric Research, Xi'an Jiaotong University, Xi'an 710049, Shaanxi, P. R. China.
c. Henry Moseley X-ray Imaging Facility, The Henry Royce Institute, School of Materials, The University of Manchester, Manchester M13 9PL, United Kingdom.
d. Department of Materials Science and Engineering, Iowa State University, Ames, IA 50011, USA.
e. Christian Doppler Laboratory for Advanced Ferroic Oxides, Sheffield Hallam University, Sheffield S1 1WB, United Kingdom.
f. Ames Laboratory, U.S. Department of Energy, Ames, IA 50011, USA.

**Figures:**

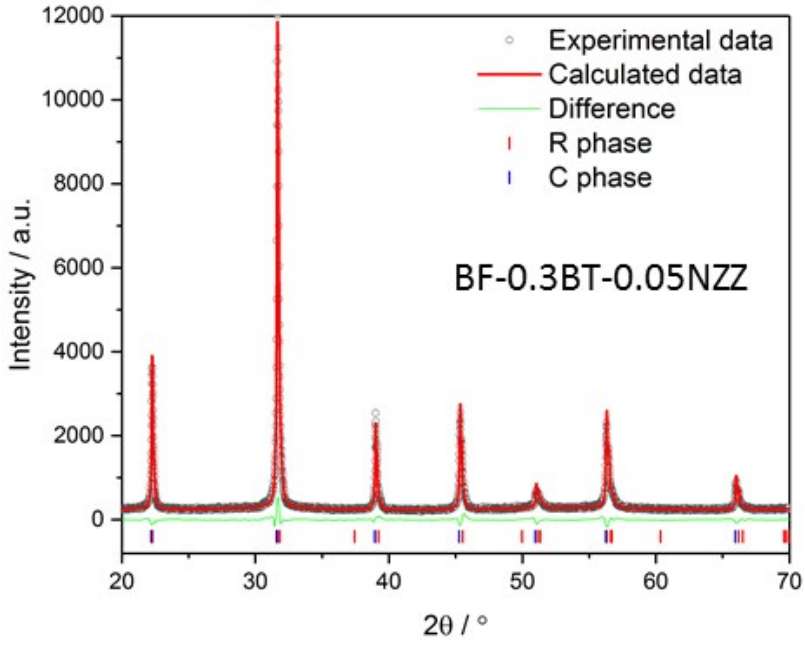


**Figure S1.** Full-pattern fitting data for BF-0.3BT-0.05NZZ ceramic powder using mixed-phase of R(*R3c*) and C($Pm\bar{3}m$).

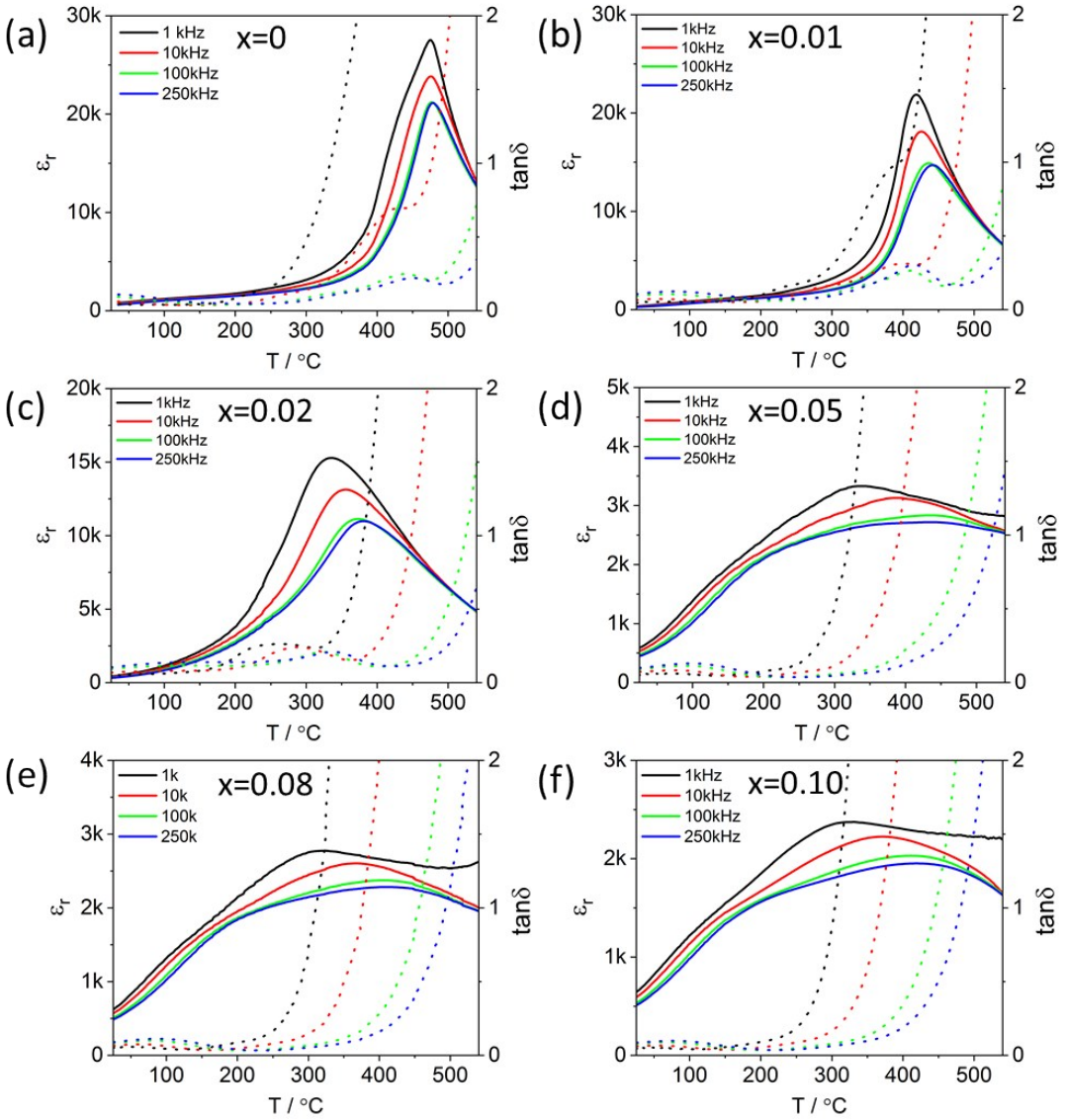


**Figure S2**. Frequency-dependent dielectric permittivity ($\varepsilon_r$-T) and loss (tanδ-T) curves for (0.7-x)BF-0.3BT-xNZZ.

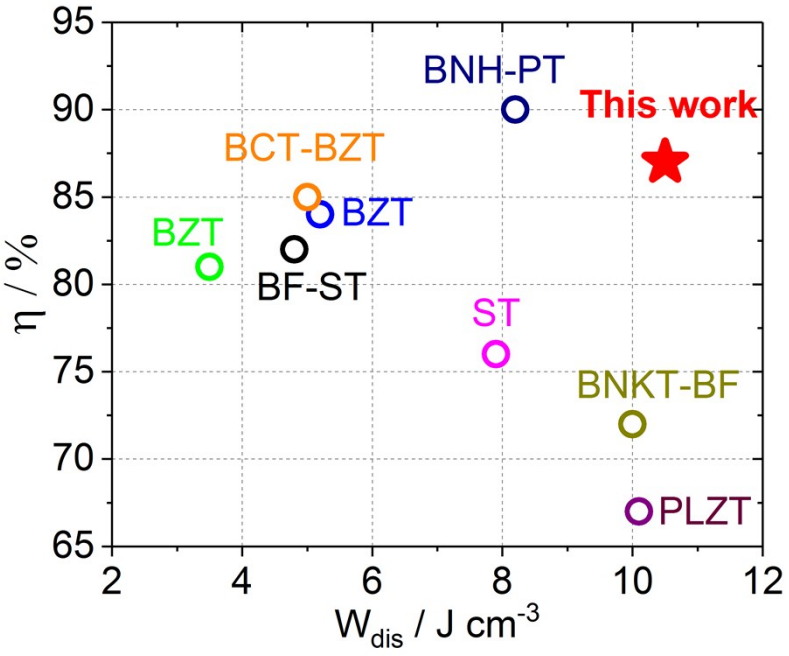


**Figure S3**. Comparison of η vs. $W_{dis}$ among different ceramic thin films and 0.62BF-0.3BT-0.08NZZ multilayers. [53-60]

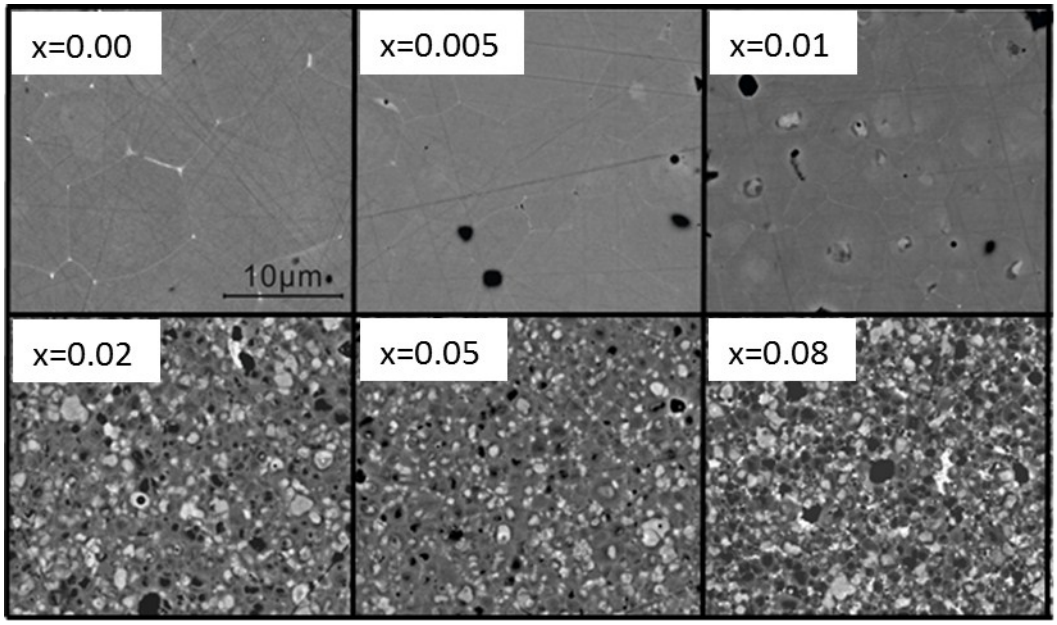


**Figure S4.** The BSE micrographs of polished surfaces for (0.7-x)BF-0.3BT-xBZZ ($0.00 \leq x \leq 0.08$).

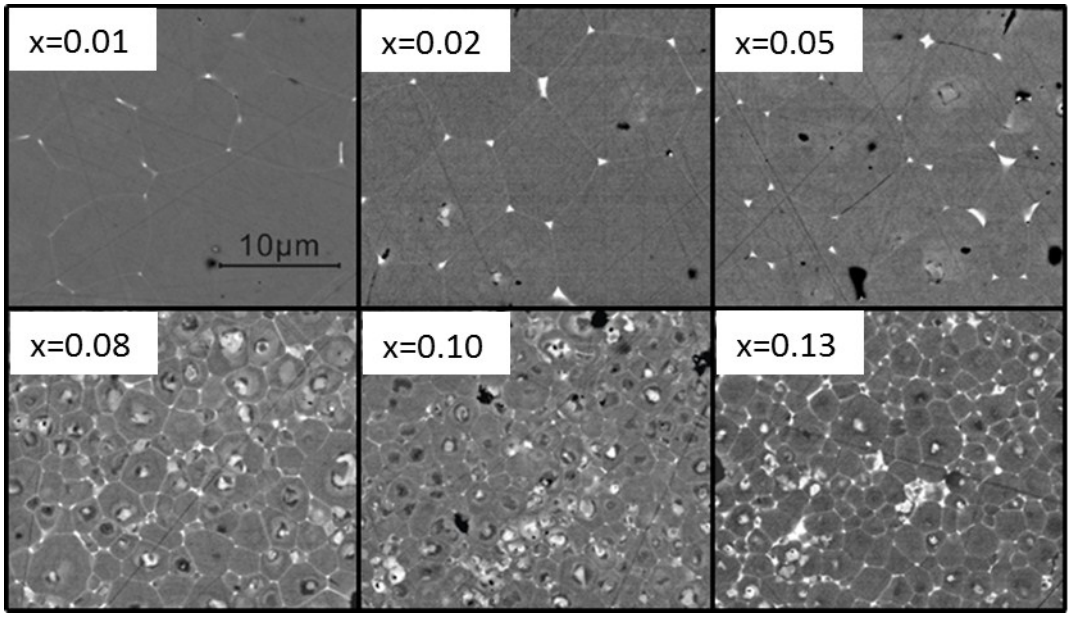


**Figure S5.** The BSE micrographs of polished surfaces for (0.7-x)BF-0.3BT-xNMN (0.01≤x≤0.13).

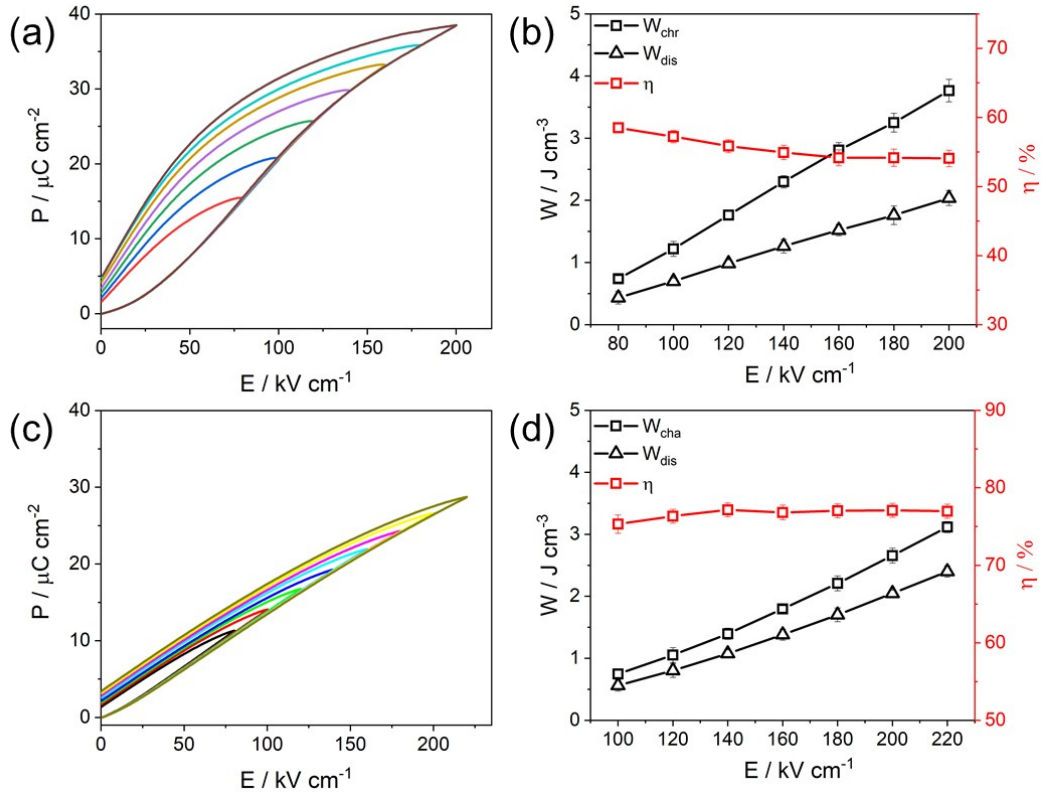


**Figure S6.** The unipolar P-E loops under $E_{max}$ for (a) BF-BT-0.05BZZ (c) BF-BT-0.10NMN; The changes of $W_{cha}$, $W_{dis}$ and η values under different electric field for (a) BF-BT-0.05BZZ (b) BF-BT-0.10NMN ceramics.

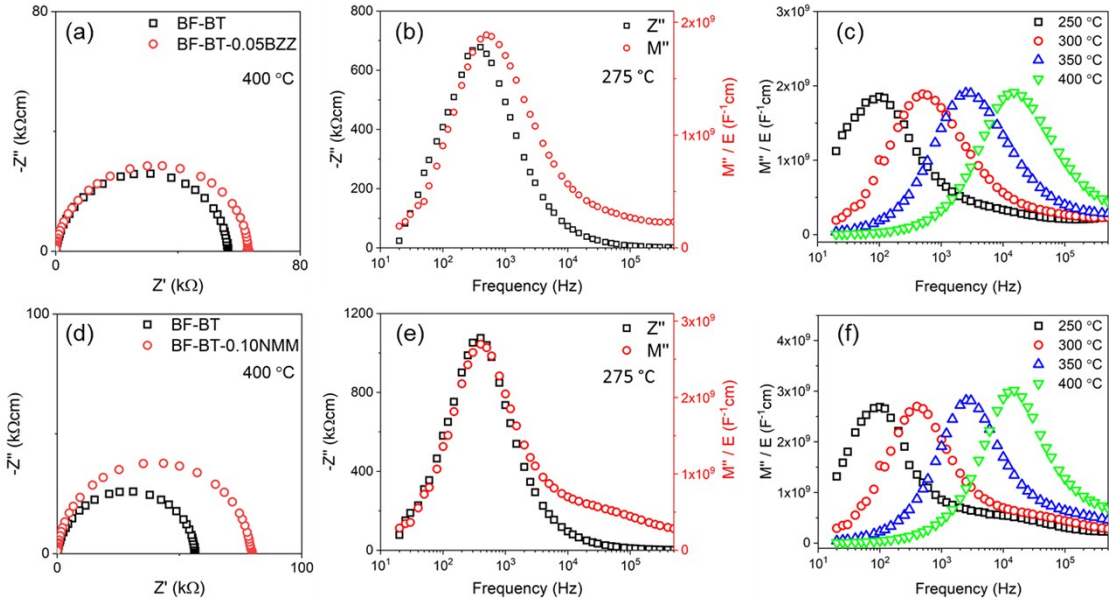


**Figure S7.** Z’ and Z’’ plot for (a) BF-BT-0.05BZZ and (d) BF-BT-0.10NMN ceramics; Combined Z’’ and M’’ spectroscopic plots at 275 $^{o}$C for (b) BF-BT-0.05BZZ and (e) BF-BT-0.10NMN ceramics; Temperature-dependent M$^{''}$- *f* spectroscopic plots for (c) BF-BT-0.05BZZ and (f) BF-BT-0.10NMN ceramics.

**Supplementary information tables:**

| | white Core | Dark core | Grey Shell | GB Phase | Overall |
|---|---|---|---|---|---|
| Bi | 19.25% | 13.95% | 14.15% | 30.4% | 15.34% |
| Fe | 17.95% | 13.73% | 13.63% | 4.8% | 14.78% |
| Ba | 4.92% | 9.06% | 11.10% | 2.8% | 7.08% |
| Ti | 4.14% | 6.66% | 9.10% | 2.7% | 6.29% |
| Results | Bi,Fe-rich | Ba,Ti-rich | Ba,Ti-rich | Bi-rich | N/A |

**Table S1.** Atomic percentage (excl. O) of BF-BT-0.08 NZZ quantified from EDS spectra from the ringed regions in Figure 2.

| Compositions | Space group | Lattice parameters / Å | | | Phase fraction / % | $R_{wp}$ | GOF |
|---|---|---|---|---|---|---|---|
| | | a | b | c | | | |
| x=0.00 | *R3c* | 5.6208(3) | 5.6208(5) | 13.8782(7) | 75.2 | 6.77 | 1.85 |
| | $Pm\bar{3}m$ | 3.9957(5) | 3.9957(8) | 3.9957(9) | 24.8 | | |
| x=0.01 | *R3c* | 5.6261(1) | 5.6261(9) | 13.8995(5) | 65.5 | 9.92 | 1.44 |
| | $Pm\bar{3}m$ | 3.9980(9) | 3.9980(3) | 3.9980(10) | 34.5 | | |
| x=0.03 | *R3c* | 5.6235(7) | 5.6235(7) | 13.9131(9) | 51.1 | 8.56 | 1.62 |
| | $Pm\bar{3}m$ | 3.9988(7) | 3.9988(5) | 3.9988(7) | 48.9 | | |
| x=0.05 | *R3c* | 5.6283(8) | 5.6283(9) | 13.9728(5) | 24.3 | 7.43 | 1.56 |
| | $Pm\bar{3}m$ | 4.0025(11) | 4.0025(9) | 4.0025(12) | 75.7 | | |
| x=0.08 | *R3c* | 5.6294(10) | 5.6294(11) | 13.9567(10) | 14.9 | 8.15 | 1.76 |
| | $Pm\bar{3}m$ | 4.0076(5) | 4.0076(7) | 4.0076(8) | 85.1 | | |
| x=0.10 | *R3c* | 5.6275(12) | 5.6275(13) | 13.9614(12) | 10.7 | 6.93 | 1.88 |
| | $Pm\bar{3}m$ | 4.0105(7) | 4.0105(8) | 4.0105(6) | 90.3 | | |

**Table S2.** Refined structural parameters of BF-BT-xNZZ ceramics.